Method for Determining the Kinetic Parameters in Diffusion-Controlled Free-Radical Homopolymerizations

Michael D. Goodner, Hyun R. Lee, and Christopher N. Bowman*

Department of Chemical Engineering, University of Colorado, Campus Box 424, Boulder, Colorado 80309-0424

Free-radical homopolymerizations of 2-hydroxyethyl methacrylate (HEMA) and diethylene glycol dimethacrylate (DEGDMA) photoinitiated by 2,2-dimethoxy-2-phenylacetophenone (DMPA) were studied. A novel analytical method for elucidating the free-volume dependencies of the propagation and termination kinetic constants from a single set of kinetic data is developed. The polymerization is divided into four regimes, nondiffusion limited, autoacceleration, reaction−diffusion without propagation limitations, and autodeceleration, in order to glean the parameters that describe the free-volume dependency. The parameters found via this method are used in a concurrently developed model to predict the polymerization rates and kinetic constant evolution throughout the polymerization. The rates and kinetic constants predicted by the model agree well with the experimentally determined rates and kinetic constants.

Introduction

Free-radical homopolymerizations of monomers that produce both linear and cross-linked polymer systems can show several distinctive features. Viscous and vitrification effects in bulk polymerizations produce autoacceleration, autodeceleration, and incomplete functional group conversion. Alternate termination mechanisms such as reaction−diffusion-controlled termination further complicate matters. In order to properly model and control these polymerizations, the kinetic behavior must be characterized throughout the course of the reaction. This work builds on previous models for this complex behavior and outlines a method for determining the kinetic parameters as a function of fractional free volume and thus conversion.

The method presented here determines the free-volume dependence of both the propagation kinetic constant (k_p) and the termination kinetic constant (k_t) from a single set of rate vs conversion kinetic data. The reaction−diffusion termination mechanism is incorporated into the expression for k_t, and thus, termination undergoes a smooth transition from diffusion-controlled to reaction−diffusion-controlled termination. The method also helps to identify the regions of autoacceleration, reaction−diffusion, and autodeceleration.

During polymerization, the conversion of monomer to polymer generally results in an increase in viscosity. This increase, in turn, causes a decrease in both the translational diffusion of monomer and polymer and the segmental diffusion of the polymer. When the diffusional limitations become large enough to restrict the diffusion of growing polymer chains, the termination rate by combination or disproportionation will decrease, causing a buildup in radical concentration and, hence, autoacceleration.

Once termination drops below a certain level, a different mechanism will become dominant: reaction−diffusion. Reaction-diffusion-controlled termination is the result of double-bond mobility in systems where growing chain-end radicals are relatively immobile. As opposed to two radicals diffusing, meeting, and reacting, reaction−diffusion termination occurs when a radical is more mobile by propagating through monomeric (or pendant) double bonds until it encounters another radical. The two radicals will then terminate through a normal bimolecular mechanism. Since the key step in the termination mechanism relies on radical propagation through monomeric double bonds, the termination kinetic constant becomes proportional to the product of the propagation kinetic constant and the double-bond concentration.

As conversion and viscosity continue to increase, the mobility in the system will reduce to a point at which the diffusion of the unreacted double bonds is limited. At this point, k_p and, consequently, the rate of polymerization drop. This effect is known as autodeceleration. The polymerization rate will quickly fall to a negligible (albeit non-zero and ever-decreasing (Kloosterboer, 1988)) value.

Several models have attempted to portray this kinetic behavior. A widely used model, proposed by Marten and Hamielec (1978, 1982), included the free-volume dependence of both k_p and k_t. Though originally proposed for reactions of bifunctional monomers, the model has also been applied to cross-linking systems (Bowman and Peppas, 1991). Soh and Sundberg (1982) used a similar free-volume approach in developing a model that incorporated radical mobility through propagation.

The flaw in the aforementioned models is that each regime in the polymerization had to be treated separately. Different equations had to be used for autoacceleration, reaction−diffusion, and autodeceleration. This problem has been solved by combining the different termination and propagation mechanisms through a summation of reaction resistances (Anseth and Bowman, 1993; Buback et al., 1989; Buback, 1990). The resulting model is comprised of one equation each for termination and propagation. These relationships (Anseth and Bowman, 1993) will be the crux of this study. Slightly rewritten with a different definition of the reaction−diffusion proportionality parameter, these equations appear as

$$k_p = \frac{k_{p0}}{1 + e^{A_p(1/f - 1/f_{cp})}} \quad (1)$$

* Phone: (303) 492-3247. Fax: (303) 492-4341. E-mail: bowmanc@colorado.edu.

S0888-5885(96)00538-6 CCC: $14.00

$$k_t = k_{t0}\left(1 + \frac{1}{\frac{Rk_p[M]}{k_{t0}} + e^{-A_t(1/f - 1/f_{ct})}}\right)^{-1} \quad (2)$$

where k_{p0} and k_{t0} are the preexponential factors, f is the fractional free volume, and f_{cp} and f_{ct} are the critical fractional free volumes at which propagation and termination, respectively, start to be diffusionally controlled. A_p and A_t are parameters which govern the rate at which propagation and termination decrease in the diffusion-controlled regions. R is the reaction−diffusion parameter, defined in this work as the termination kinetic constant in the reaction−diffusion region divided by the product of the propagation kinetic constant and the instantaneous unreacted functional group concentration, [M]. Note that k_{p0} and k_{t0} are the true values of the propagation and termination kinetic constants in the absence of diffusional limitations.

This paper utilizes eqs 1 and 2 in a method for determining the kinetic constant dependencies on free volume from a single set of kinetic data, unlike other methods which utilize unsteady-state reactions to uncouple k_p and k_t and do not explicitly determine the free-volume-associated parameters. The parameters found will be used in a simulation developed by Kannurpatti et al. (1997), and the simulated rate data will be compared to the experimentally generated data. The model assumes pseudosteady state (rate of initiation equal to the rate of termination), constant initiator efficiency, and equilibrium volume shrinkage.

Experimental Section

The bifunctional monomer used in this study, 2-hydroxyethyl methacrylate (HEMA), was obtained from Aldrich (Milwaukee, WI) and dehibited to remove the inhibitor (hydroquinone monomethyl ether). The tetrafunctional diethylene glycol dimethacrylate (DEGDMA) was obtained from Polysciences (Warrington, PA) and used as received. The photoinitiator used in this study, 2,2-dimethoxy-2-phenylacetophenone (DMPA), was obtained from Ciby-Geigy (Hawthorne, NY) and used as received.

The kinetic experiments were performed in a differential scanning calorimeter (DSC). For the photopolymerizations, a dual-beam photocalorimetric accessory (DPA) equipped with a monochrometer supplied 365-nm ultraviolet light of approximately 4 mW/cm^2. The rate of polymerization was determined by monitoring the heat evolved in the exothermic reactions. The standard heat of polymerization is −13.1 kcal/mol for methacrylates (Cook, 1992). For the photopolymerizations, a DMPA concentration of 0.5 wt % was used with small 2−3 mg samples, in order to adhere to the thin-film approximation for initiation rate. Reactions were carried out at 30 °C, and the samples were purged in the DSC with dry nitrogen prior to and throughout the reaction to prevent oxygen inhibition.

Analytical Method

To analyze the kinetic data and obtain the parameters in eqs 1 and 2, the polymerization can be broken up into four regions: (i) the "normal" polymerization region with no diffusional controls; (ii) the autoacceleration region, in which termination is diffusion controlled but propagation is not; (iii) the reaction−diffusion termination region, with constant k_p; and (iv) the autodeceleration region with termination still reaction−diffusion controlled. These regions, along with the physical properties characterizing them, are summarized in Table 1. The standard rate equation for radical polymerizations will be the starting point for analysis in each region. By applying the pseudosteady-state assumption requiring the rate of initiation to equal the rate of termination, the radical concentration can be eliminated. This leaves the rate of polymerization as

Table 1. Physical Description of the Four Regions Examined by the Analytical Method

region	phys descriptn	free vol	reaction−diffusion?
i	no diffusional limitations on either propagation or termination	$f \gg f_{cp}, f_{ct}$	no
ii	autoacceleration	$f_{ct} > f \gg f_{cp}$	no
iii	reaction−diffusion-controlled termination, propagation not diffusion limited	$f_{ct} > f \gg f_{cp}$	yes
iv	autodeceleration with reaction−diffusion controlled termination	$f < f_{ct}, f_{cp}$	yes

$$R_p = \left(\frac{R_i}{2}\right)^{1/2} \frac{k_p}{k_t^{1/2}}[M] \quad (3)$$

where R_i is the rate of initiation of radicals.

Additionally, the functional group conversion and the fractional free volume can be related through a series of equations:

$$f = f_m\phi_m + f_p(1 - \phi_m) \quad (4)$$

$$\phi_m = \frac{1 - X}{1 - X + \frac{\rho_m}{\rho_p}X} \quad (5)$$

$$f_m = 0.025 + \alpha_m(T - T_{gm}) \quad (6)$$

$$f_p = 0.025 + \alpha_p(T - T_{gp}) \quad (7)$$

In these equations, f_m and f_p are the fractional free volumes of pure monomer and pure polymer, ϕ_m is the volume fraction of monomer, and the α's, T_g's, and ρ's are the coefficients of expansion, glass transition temperatures, and densities, respectively, of the pure monomer and polymer components. T represents the temperature at which the polymerization is carried out. These relationships follow those used in the development of eqs 1 and 2.

To determine the kinetic parameters without having to know other parameters *a priori*, the regions in which reaction−diffusion termination occurs (regions iii and iv) will be examined first. At small values of f (i.e., $f \ll f_{ct}$), the reaction−diffusion term dominates, and thus, k_t can be represented as

$$k_t = Rk_p[M] \quad (8)$$

Under this condition, the rate of polymerization becomes

$$R_p = \left(\frac{R_i k_p[M]}{2R}\right)^{1/2} \quad (9)$$

Two different situations can occur when reaction−diffusion termination dominates. If propagation is not diffusion limited ($f \gg f_{cp}$), k_p can be approximated by k_{p0}. This is region iii and will be referred to as the reaction−diffusion region. Rearranging eq 9 after approximating k_p, we can define the quantity

$$\gamma \equiv \frac{2R[\mathrm{M}]_0 {R_\mathrm{N}}^2}{R_\mathrm{i}(1-X)} = k_\mathrm{p}^0 \tag{10}$$

In this and subsequent definitions, $[\mathrm{M}]_0$ is the initial functional group concentration, R_N is the normalized rate of polymerization in s^{-1} (dimensional rate divided by $[\mathrm{M}]_0$), and the $1 - X$ term comes from the relation between initial and instantaneous unreacted functional group concentration: $[\mathrm{M}] = [\mathrm{M}]_0(1 - X)$.

Thus, when termination occurs by reaction−diffusion but propagation is not diffusion limited, the quantity γ will be constant at a value of k_{p0}. By plotting γ vs conversion or fractional free volume, k_{p0} can easily be determined (if this situation occurs during the polymerization). Note that the reaction−diffusion constant, R, must be known beforehand.

The second situation occurring when termination occurs by reaction−diffusion is the autodeceleration region. In this case (iv), the expression for k_p from eq 1 cannot be simplified. Squaring the rate equation, rearranging, and taking the natural logarithm leads to

$$\delta \equiv \ln\left[\frac{R_\mathrm{i}k_{p0}(1-X)}{2R[\mathrm{M}]_0{R_\mathrm{N}}^2} - 1\right] = A_\mathrm{p}\frac{1}{f} - \frac{A_\mathrm{p}}{f_{cp}} \tag{11}$$

Thus, plotting δ vs $1/f$ will provide A_p from the slope and f_{cp} from the intercept. Note that k_{p0} appears in the definition of δ, but since it has already been determined from iii, A_p and f_{cp} can be found explicitly.

Next, region i can be analyzed. Since there are no diffusional limitations, k_p and k_t can be approximated by their preexponential values, k_{p0} and k_{t0}. Rearranging eq 3 gives the parameter α:

$$\alpha \equiv \sqrt{\frac{2}{R_\mathrm{i}}}\frac{R_\mathrm{N}}{1-X} = \frac{k_{p0}}{{k_{t0}}^{1/2}} \tag{12}$$

In region i, α will remain constant. Using the value for k_{p0} determined in region iii, k_{t0} can now be found.

Lastly, the autoacceleration region can be analyzed similarly to region iv. In this region, $f_{cp} \ll f < f_{ct}$, so k_p can once again be approximated by k_{p0}. During autoacceleration, termination is governed by diffusional limitations while reaction−diffusion is still negligible. Under these circumstances, the expression for k_t will reduce to

$$k_\mathrm{t} = \frac{k_{t0}}{1 + \mathrm{e}^{A_t(1/f - 1/f_{ct})}} \tag{13}$$

Following the same analytical path as in region iv leads to the definition of β:

$$\beta \equiv \ln\left[\frac{2k_{t0}{R_\mathrm{N}}^2}{R_\mathrm{i}{k_{p0}}^2(1-X)^2} - 1\right] = A_\mathrm{t}\frac{1}{f} - \frac{A_\mathrm{t}}{f_{ct}} \tag{14}$$

By plotting β vs $1/f$, the last two parameters, A_t and f_{ct}, can be determined.

Table 2. Material and Kinetic Properties for HEMA and DEGDMA[a]

Material Properties for HEMA		
$\rho_m = 1.073$ g/cm^3	$\rho_p = 1.15$ g/cm^3	$[\mathrm{M}]_0 = 8.2$ mol/L
$T_{gm} = -60$ °C	$T_{gp} = 55$ °C	
$\alpha_m = 0.0005$ °C^{-1}	$\alpha_p = 0.000\ 075$ °C^{-1}	
Material Properties for DEGDMA		
$\rho_m = 1.061$ g/cm^3	$\rho_p = 1.32$ g/cm^3	$[\mathrm{M}]_0 = 8.7$ mol/L
$T_{gm} = -100$ °C	$T_{gp} = 225$ °C	
$\alpha_m = 0.0005$ °C^{-1}	$\alpha_p = 0.000\ 075$ °C^{-1}	
Kinetic Parameters for HEMA		
$R = 4$		
$k_{p0} = 1000$ L/mol·s	$A_p = 0.66$	$f_{cp} = 0.042$
$k_{t0} = 1.1 \times 10^6$ L/mol·s	$A_t = 1.2$	$f_{ct} = 0.060$
Kinetic Parameters for DEGDMA		
$R = 2$		
$k_{p0} = 200$ L/(mol·s)	$A_p = 1.2$	$f_{cp} = 0.062$
$k_{t0} = 8.0 \times 10^4$ L/(mol·s)	$A_t = 2.7$	$f_{ct} = 0.089$

[a] The reaction−diffusion parameters, R, are from C. N. Bowman (unpublished data).

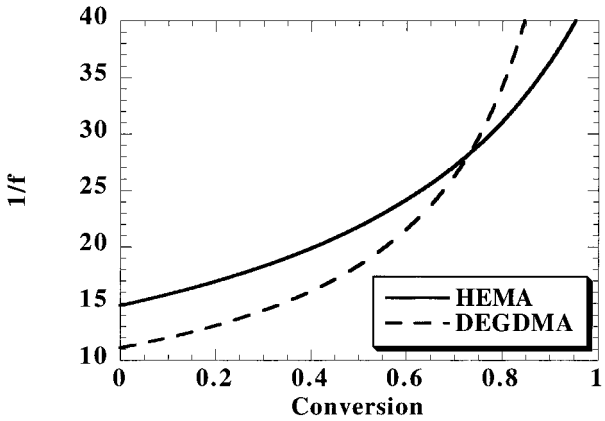

Figure 1. Relationship between the inverse fractional free volume and conversion of the HEMA and DEGDMA systems. Curves are generated from eqs 4−7.

Through this analysis, k_{p0}, k_{t0}, A_p, A_t, f_{cp} and f_{ct}, can be determined. The values for the systems studied here can be found in Table 2. Only the reaction−diffusion parameter R needs to be known beforehand. This parameter can be found easily from unsteady-state reactions (Anseth et al., 1994a−c). Some systems will not have a well-defined region iii. In this case, two approaches can be taken to find k_{p0}: it either can be estimated from the nonconstant γ value between regions ii and iv (the method used in this study), or k_{p0} can be found directly from the unsteady-state analysis necessary to determine R.

Results and Discussion

Since the analysis is carried out in the autoacceleration and autodeceleration regions as a function of inverse fractional free volume, the results reported here will be presented with inverse fractional free volume as the independent variable. Figure 1 shows the relationship between $1/f$ and functional group conversion. These curves are developed from eqs 4−7. Note that the rise in $1/f$ at high conversions is much steeper for the DEGDMA system than it is for HEMA; this feature is due to the lower polymer fractional free-volume value for DEGDMA (0.010 as opposed to 0.023 for HEMA), which results from the higher glass transition temperature for poly(DEGDMA).

Figures 2 and 3 compare simulated rate data to experimental data for both HEMA and DEGDMA and

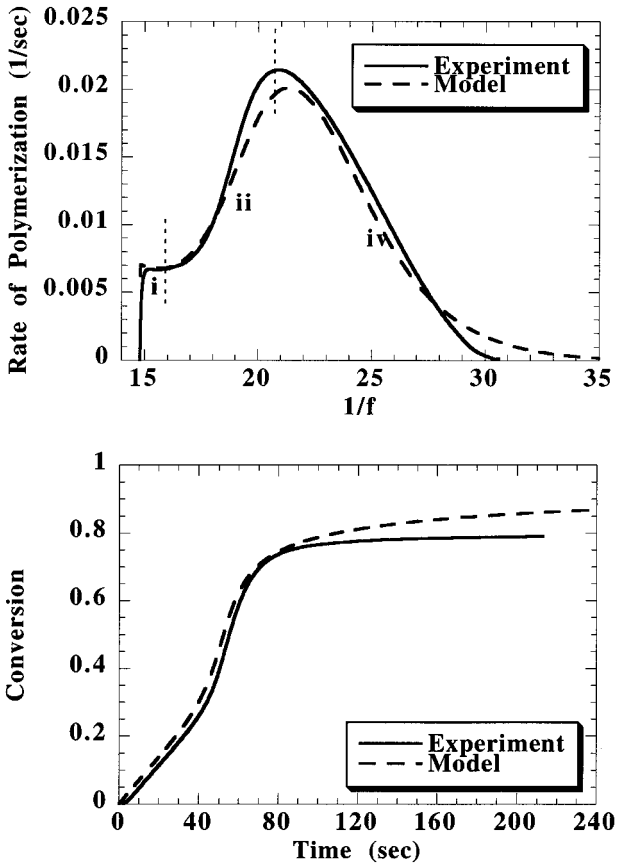

Figure 2. (a, top) Comparison of the experimental and simulated rate curves for HEMA polymerization with kinetic regions delineated: (i) no diffusion limitations to propagation or termination, (ii) autoacceleration, and (iv) autodeceleration. (b, bottom) Conversion vs time curves for the HEMA polymerization and simulation shown in a.

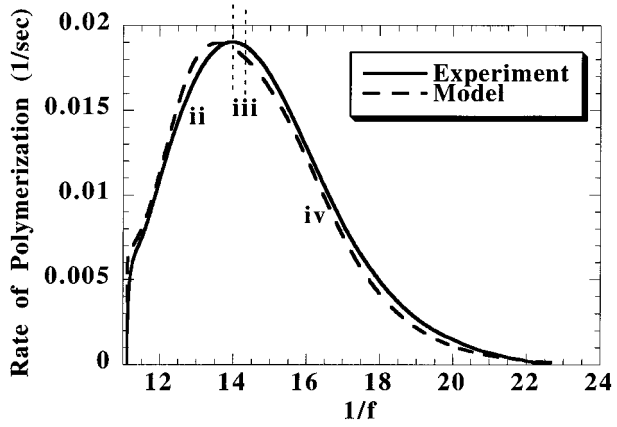

Figure 3. Comparison of the experimental and simulated rate curves for DEGDMA polymerization with kinetic regions delineated: (ii) autoacceleration, (iii) reaction−diffusion termination without propagation limitations, and (iv) autodeceleration.

delineate the different kinetic regions encountered in the polymerization. Figure 2a shows the HEMA polymerization. At the start of the polymerization, when there are no diffusional controls on either propagation or termination, the normalized rate of polymerization is approximately constant. The experimental curve shows a small start-up period in which the DSC is establishing thermal equilibrium after ignition of the UV light source. In the autoacceleration region, the rate increases greatly as termination decreases and living polymer chains are allowed to exist longer and in greater quantities. The simulation tracks the rate well; the value and location of the maximum rate of polymerization are both reproduced to within a few percent.

As the reaction−diffusion termination mechanism starts to dominate, propagation becomes diffusion limited and the system starts to autodecelerate. Thus, when the fractional free volumes for propagation limitation and reaction−diffusion dominance are close together, region iii (pure reaction−diffusion termination without propagation limitation) will be ill-defined or absent. The simulation captures this behavior excellently; the decrease in rate with fractional free volume is mimicked almost exactly. Note that the simulation captures the end of the polymerization with a tail extending out to $1/f \approx 35$. This is not seen in the experiments, as the DSC has trouble capturing the low but obviously still finite polymerization rate that occurs at high conversions. The difficulty of the DSC in monitoring the low rates is associated with the small heat-release rates.

Figure 2b presents the same data for the HEMA polymerization in a different fashion: as a conversion vs time graph. The agreement between simulation and experiment is startling. The model splendidly reproduces the polymerization through autoacceleration and autodeceleration, up to $t = 80$ s. The slight shift to the left of the model curve results from the DSC start-up discussed previously. The impact of rates near the limit of DSC detection at the high conversions can clearly be seen, as the two curves diverge slightly after 80 s.

Figure 3 shows the rate vs inverse fractional free-volume behavior for the DEGDMA system. Due to the multifunctional nature of DEGDMA, creation of microgel regions occurs at very low conversions (Anseth et al., 1995), which immediately limits the termination in the system. As a result, the polymerization starts in the autoacceleration mode. The model reproduces the normalized rate well, with the same difference in start-up that was seen in Figure 2a for the HEMA polymerization. At the end of autoacceleration, the maximum rate is reproduced very accurately, and the fractional free volume of maximum rate is accurate to within a few percent.

When reaction−diffusion termination begins to govern, the same problem occurs for DEGDMA that occurred for HEMA, namely, a nearly immediate drop in propagation. The reaction−diffusion region is small but present in the DEGDMA polymerization, as opposed to completely absent as in the HEMA scenario. The simulation tracks the rate excellently through reaction−diffusion and autodeceleration.

We will now take a closer look at the analytical method used to find the kinetic parameter values for HEMA and DEGDMA listed in Table 2 and used in the simulation for generation of Figures 2 and 3. The first region analyzed is region iii, reaction−diffusion with no propagation limitations. As seen in Figures 2 and 3, this region is absent in the case of HEMA and ill-defined for DEGDMA. For this study, the value of γ (and therefore k_{p0}) was estimated using the autoacceleration-to-autodeceleration transition, where reaction−diffusion would normally occur.

Next, δ is plotted vs $1/f$ in Figure 4 for the autodeceleration region in the HEMA polymerization. The slope and intercept provide A_p and f_{cp}, respectively. δ has some curvature in this region, but it does not influence the determination of A_p and f_{cp} greatly, and not all systems show this behavior. The curvature demonstrated in Figure 4 is likely caused by an incom-

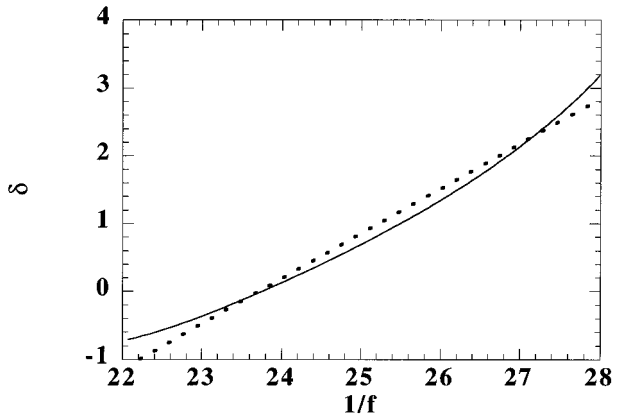

Figure 4. Determination of A_p and f_{cp} in region iv, autodeceleration, for the HEMA polymerization. The solid line represents the experimental data, while the dashed line represents the fit of eq 11 to the data.

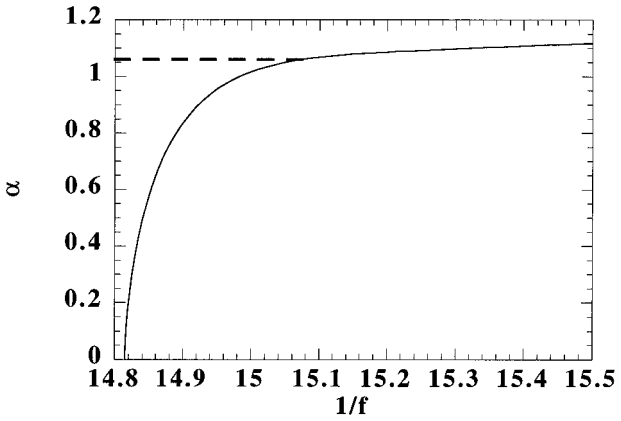

Figure 5. Parameter α at the start of the HEMA polymerization. The dashed line indicates the value α = 1.06 used to determine k_{t0} via eq 12.

plete dominance of reaction−diffusion at lower conversion (lower 1/*f*).

Similar analyses are performed in the nonlimited and autoacceleration regions. In the case of nonlimited propagation and termination (Figure 5), α is shown vs 1/*f* at the start of the polymerization. After the start-up phenomenon associated with the DSC, α assumes an approximately constant value. There is a slight increase which likely reflects slightly increased viscosity and, therefore, slightly reduced termination around growing active centers. Upon determination of α, k_{t0} may be calculated from eq 12. In Figure 6, β is plotted vs 1/*f* in the autoacceleration region. The resulting fit gives A_t and f_{ct}. As opposed to δ in the autodeceleration region, β shows very little curvature, indicating that the assumption of $f_{ct} > f \gg f_{cp}$ is valid.

The parameters determined in the analysis allow determination of the kinetic constants for propagation and termination as a function of inverse fractional free volume via eqs 1 and 2. This dependence is shown in Figure 7 for the HEMA polymerization along with experimental values of k_p and k_t determined by the aftereffect experiments detailed in Kannurpatti et al. (1997). The behavior k_p displays is rather straightforward. It maintains a constant value up to $1/f \approx 22$, at which point diffusion limitations set in. It then drops approximately $1^1/_2$ orders of magnitude over the rest of the polymerization. The k_t curve shows a much more complex evolution. k_t drops quickly from its initial value, as growing polymer chains experience diffusion limitations and autoacceleration occurs. At a 1/*f* value

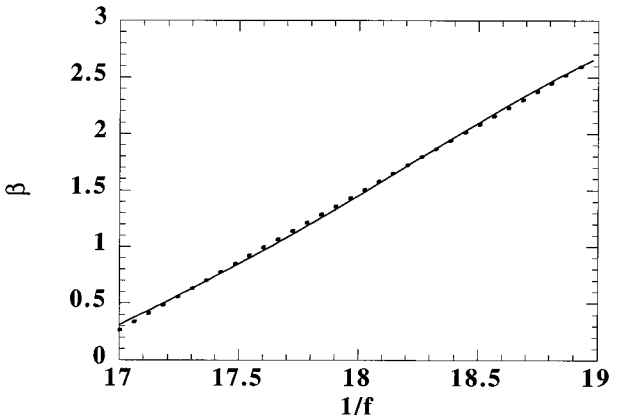

Figure 6. Determination of A_t and f_{ct} in region ii, autoacceleration, for the HEMA polymerization. The solid line represents the experimental data, while the dashed line represents the fit of eq 14 to the data.

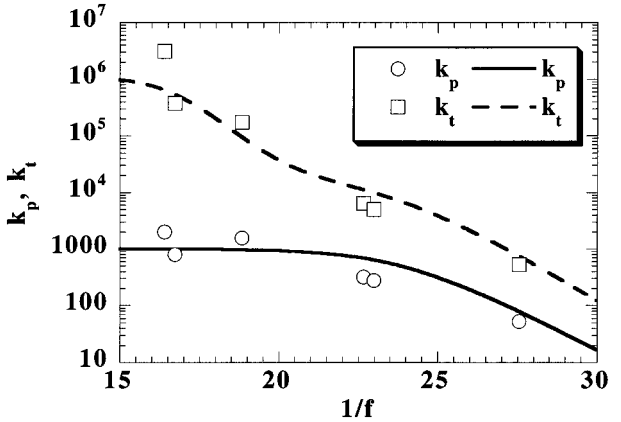

Figure 7. Experimentally determined and modeled kinetic constants for the HEMA polymerization. Modeled values are generated using eqs 1 and 2 and the parameters determined from the data described in Figures 2−6.

of approximately 20, reaction−diffusion termination starts to dominate and the decrease in k_t is curtailed greatly. This slow decrease over the range $1/f \approx 20-22$ is due to the reaction−diffusion termination being proportional to the unreacted functional group concentration, which is decreasing as the reaction proceeds. When k_p starts to drop in the autodeceleration region, k_t decreases through the reaction−diffusion proportionality. It is well worth noting that the fit of the kinetic constants in Figure 7 has no adjustable parameters—all the of parameters used were determined from the polymerization rate studies.

Conclusions

In this paper, a new method for the determination of kinetic parameters in diffusion-controlled homopolymerizations has been presented. The kinetic constants for propagation and termination are allowed to vary with fractional free volume, which allows diffusional limitations to be accounted for. The free-volume dependencies are elucidated from a single set of experimental kinetic data for two different systems: HEMA, a linear polymer-forming monomer, and DEGDMA, a monomer which forms a cross-linked polymer network. The kinetic parameters found via this analysis are unique; only one set of values can be found for a given set of rate vs conversion data. Finding these parameters from one set of kinetic data contrast other methods that require a series of unsteady-state reactions to

determine kinetic constant evolution and do not explicitly ascertain the free-volume dependence. The parameters that are found using this method are used in a simulation to predict the polymerization rates and kinetic constant evolution throughout the course of the polymerization. Agreement between the model and the experiments is excellent.

The analytical method recognizes four regimes within the polymerization: nondiffusion-limited propagation and termination, autoacceleration, reaction−diffusion termination without propagation limitations, and autodeceleration. The analysis isolates different parameters in each of the regions (Figures 3−5), which allows the free-volume dependencies to be determined from simple linearizations. This analytical method is demonstrated using photopolymerization data; however, it could equally be applied to any radical polymerization, independent of the initiation scheme, with minor changes. The parameter-determination method outlined here and the model of Kannurpatti et al. (1997) work symbiotically to provide a thorough simulation of diffusion-controlled free-radical homopolymerizations.

Acknowledgment

We acknowledge 3M and Du Pont for their support of this work and the National Science Foundation for its support of this work through the Presidential Faculty Fellowship to C.N.B. (CTS-9453369) and a graduate fellowship to M.D.G.

Literature Cited

Anseth, K. S.; Bowman, C. N. Reaction Diffusion Enhanced Termination in Polymerizations of Multifunctional Monomers. *Polym. React. Eng.* **1993**, *1*, 499.

Anseth, K. S.; Bowman, C. N.; Peppas, N. A. Polymerization Kinetics and Volume Relaxation Behavior of Photopolymerized Multifunctional Monomers Producing Highly Crosslinked Networks. *J. Polym. Sci., Polym. Chem.* **1994a**, *32*, 139.

Anseth, K. S.; Wang, C. M.; Bowman, C. N. Kinetic Evidence of Reaction Diffusion during the Polymerization of Multi(meth)-acrylate Monomers. *Macromolecules* **1994b**, *27*, 650.

Anseth, K. S.; Wang, C. M.; Bowman, C. N. Reaction behaviour and kinetic constants for photopolymerization of multi(meth)-acrylate monomers. *Polymer* **1994c**, *35*, 3243.

Anseth, K. S.; Kline, L. M.; Walker, T. A.; Anderson, K. J.; Bowman, C. N. Reaction Kinetics and Volume Relaxation during Polymerizations of Multiethylene Glycol Dimethacrylates. *Macromolecules* **1995**, *28*, 2491.

Bowman, C. N.; Peppas, N. A. Coupling of Kinetics and Volume Relaxation during Polymerization of Multiacrylates and Multimethacrylates. *Macromolecules* **1991**, *24*, 1914.

Buback, M. Free-radical polymerization up to high conversion. A general kinetic treatment. *Die Makromolek. Chem.* **1990**, *191*, 1575.

Buback, M.; Degener, B.; Huckestein, B. Conversion dependece of free-radical polymerization rate coefficients from laser-induced experiments, 1. *Makromol. Chem. Rapid Commun.* **1989**, *10*, 311.

Cook, W. D. Thermal aspects of the kinetics of dimethacrylate photopolymerization. *Polymer* **1992**, *33*, 2152.

Kannurpatti, A. R.; Goodner, M. D.; Bowman, C. N. In *Reaction Behavior And Kinetic Modeling Studies Of "Living" Radical Photopolymerizations*. ACS Symposium Series; Scranton, A. B., Ed.; American Chemical Society: Washington, DC, 1997.

Kloosterboer, J. G. Network Formation by Chain Crosslinking Photopolymerization and its Applications in Electronics. *Adv. Polym. Sci.* **1988**, *84*, 1.

Marten, F.; Hamielec, A. In *Polymerization Reactors and Processes*; Henderson, J., Bouton, T., Eds.; ACS Symposium Series 104; American Chemical Society: Washington, DC, 1978; p 43.

Marten, F. L.; Hamielec, A. E. High-Conversion Diffusion-Controlled Polymerization of Styrene. I. *J. Appl. Polym. Sci.* **1982**, *27*, 489.

Soh, S. K.; Sundberg, D. C. Diffusion-Controlled Vinyl Polymerization. I. The Gel Effect. *J. Polym. Sci., Polym. Chem.* **1982**, *20*, 1299.

Received for review August 30, 1996
Revised manuscript received November 21, 1996
Accepted November 22, 1996[⊗]

IE9605387

[⊗] Abstract published in *Advance ACS Abstracts,* February 15, 1997.